Physical Properties of the Solar Atmosphere Derived from Comparison of Spectro-Polarimetric SDO/HMI Observables with 3D Radiative MHD Simulations

Viacheslav Sadykov[1], Irina Kitiashvili[2], Alan Wray[2], Alexander Kosovichev[2,3], Isaac Asante[1], Dorsa Erfani[1]

[1]Georgia State University, [2]NASA Ames Research Center, [3]New Jersey Institute of Technology

International Astronomical Union (IAU) Symposium 365

08/21-25/2023, Yerevan, Armenia

Image credits: NASA, V. Sadykov

Introduction

- The insight into the plasma processes in the solar atmosphere comes from remote sensing. Correspondingly, it is critical to interpret remote sensing observations.
- Realistic numerical simulations of the solar atmosphere and synthesis of the plasma emission and spectra represent a reliable bridge for interpreting remote sensing observations. Examples:
  - Bifrost simulations + RH / Multi3D (Leenaarts et al. 2013, Rathore et al. 2015, etc.): information about the physical parameters in the atmosphere from Mg II, C II, and other spectral line observation.
  - StellarBox + SPINOR/STOPRO (Kitiashvili et al. 2015): interpretation of the SDO/HMI observations.
  - MURAM + Milti3D (Bjørgen et al. 2019): formation of various spectral lines in the 3D MHD model of the solar flare process.

3D RMHD Dynamo Simulations

- “StellarBox” code solves the fully compressible MHD equations with radiative transfer solved by ray-tracing and opacity binning techniques, and large-eddy simulation (LES) treatment of subgrid turbulent transport (Wray et al. 2015, 2018). The current version of the code supports option to extend the computational domain to the corona and deeper convective layers as well as in the horizontal directions.
- Initial computational setup: the computational domain of 6.4 x 6.4 x 6.2 Mm includes a 1-Mm layer of the photosphere. The grid-size is 12.5km in the horizontal directions; a variable grid-spacing of similar size is used in the vertical direction. The lateral boundary conditions are periodic. The modeling data cubes delivered with 5s cadence were analyzed. The initial seed magnetic field was a uniform vertical 0.01G field

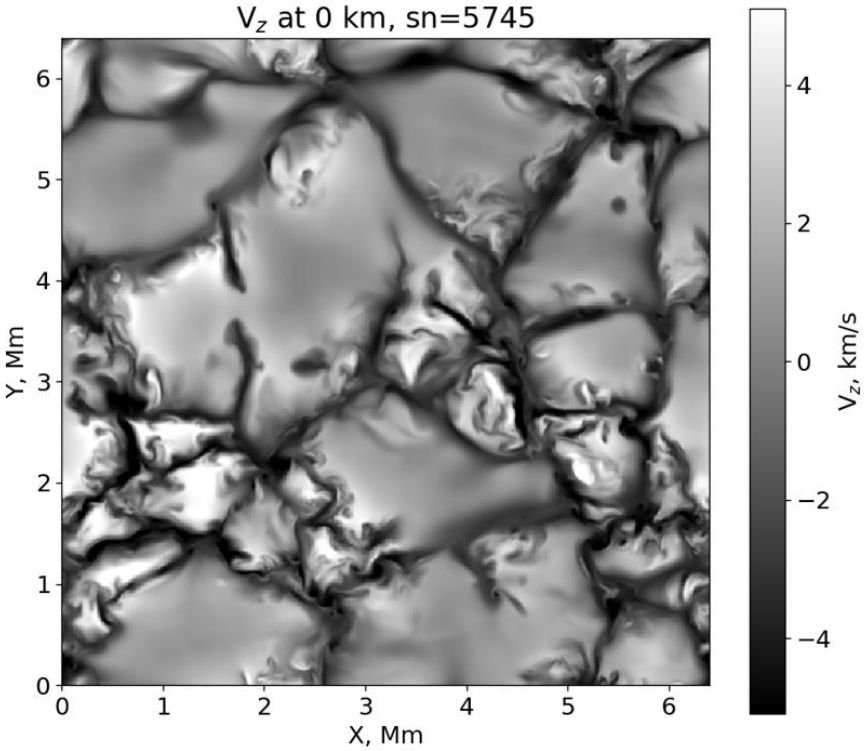

Illustration of a vertical velocity map at z = 0 Mm height for the initial time moment of the considered simulation series.

Modeling of SDO/HMI Observables

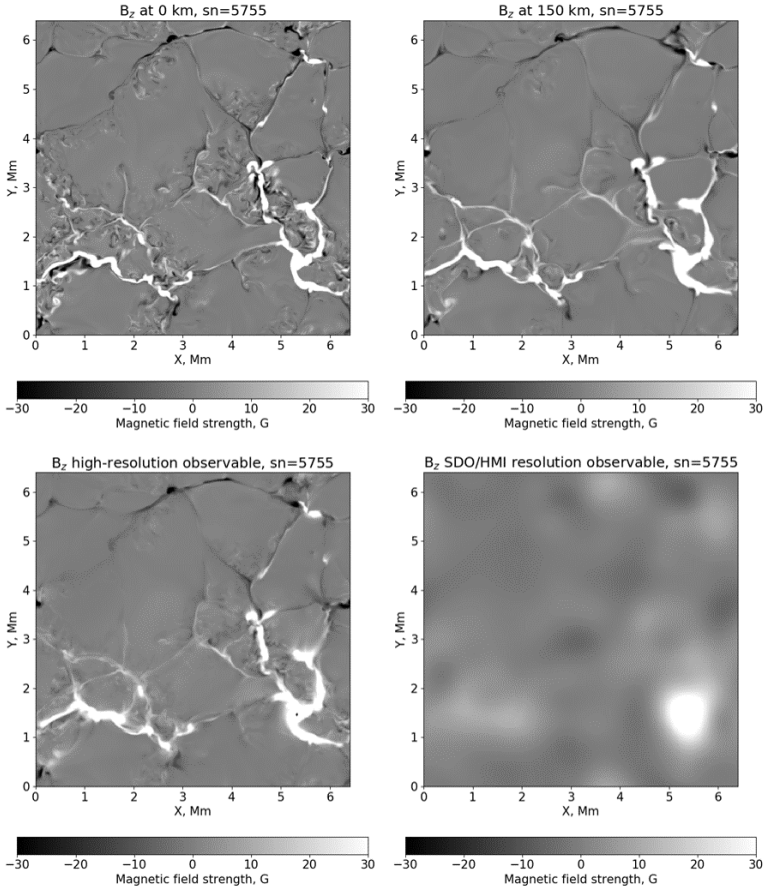

- Fe I 6173 Å synthetic Stokes profiles are computed with the SPINOR/STOPRO code in LTE approximation for 6 angles (0^o-80^o degrees), considered in both the numerical and instrumental resolutions
- The simplified Line-of-Sight (LoS) pipeline is implemented following Couvidat et al. (2016).
- The corresponding continuum intensity, line depth, Doppler velocity, and LoS magnetic field observables are derived.
- The observables are compared to the physical properties of the atmosphere.

Comparison of the vertical magnetic field maps at 0 km and 150 km heights (upper panels) with the corresponding high resolution and SDO/HMI resolution observables (lower panels) for the disk center case.

Modeling of Fe I 6173 Å Stokes profiles

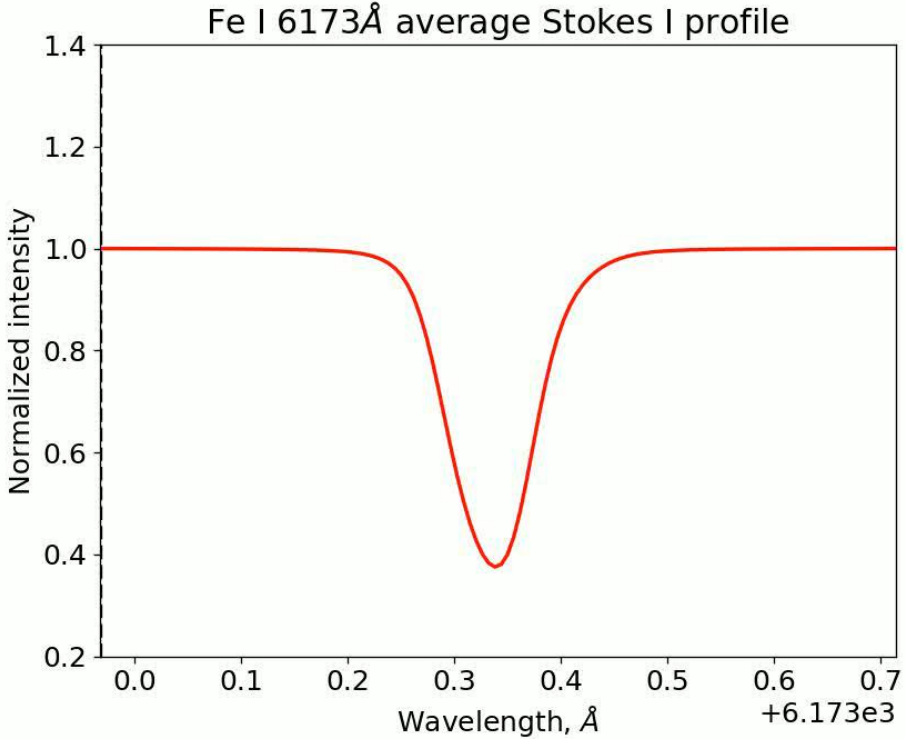

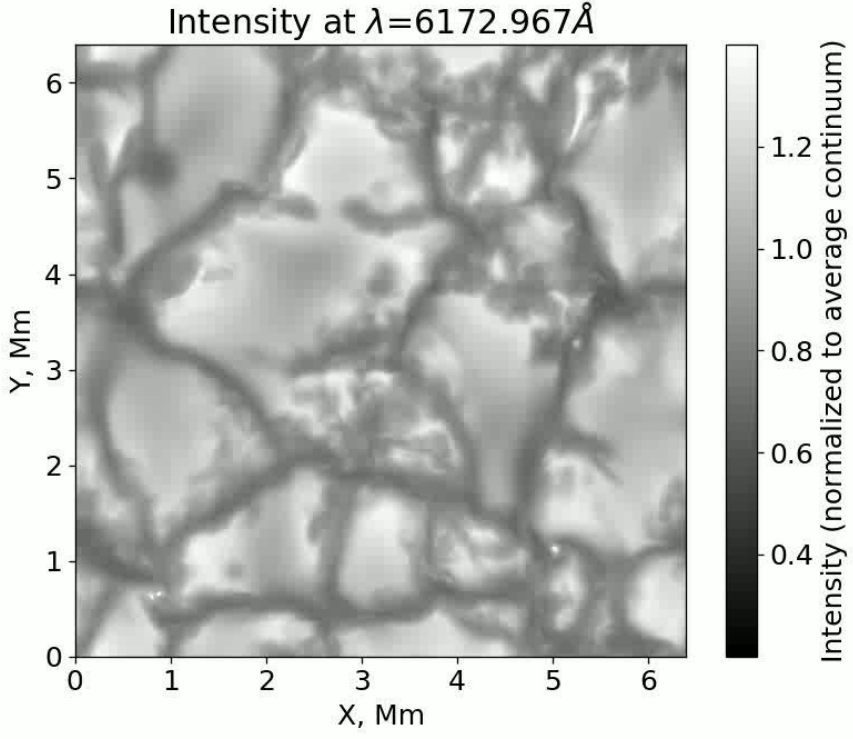

SDO/HMI B_{LOS} Observables

B_{LOS} at 0 km

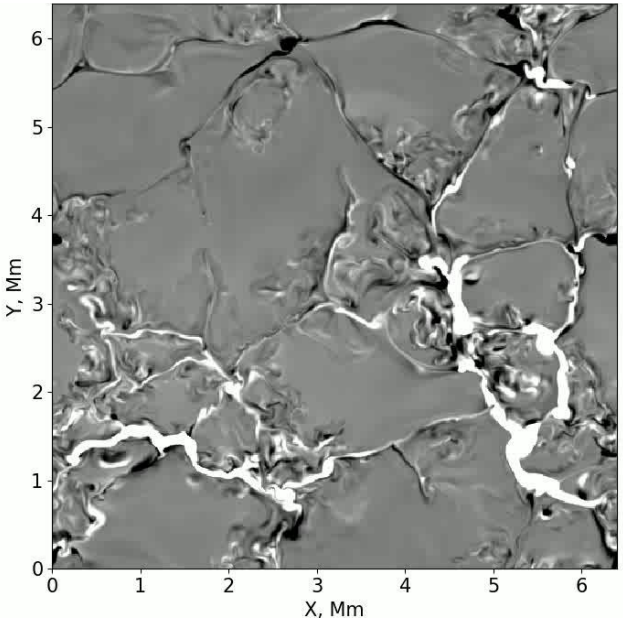

B_{LOS} observable (high res)

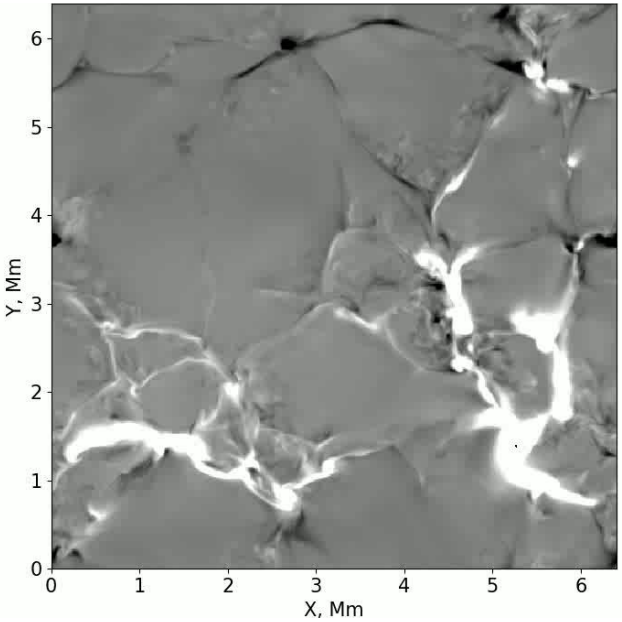

B_{LOS} observable (SDO/HMI res)

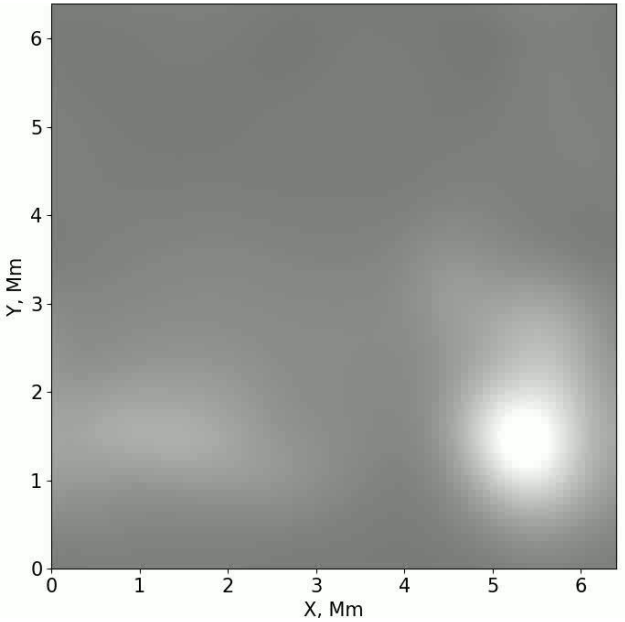

Observables and Atmospheric Properties

- To understand to which height of the atmosphere the observables are sensitive to, we calculate Pearson CC between the observables and the actual physical properties
- The line-of-sight velocity observables are unambiguously correlated with the physical quantities at certain heights for the disk center case (there is a sharp peak of the CC)

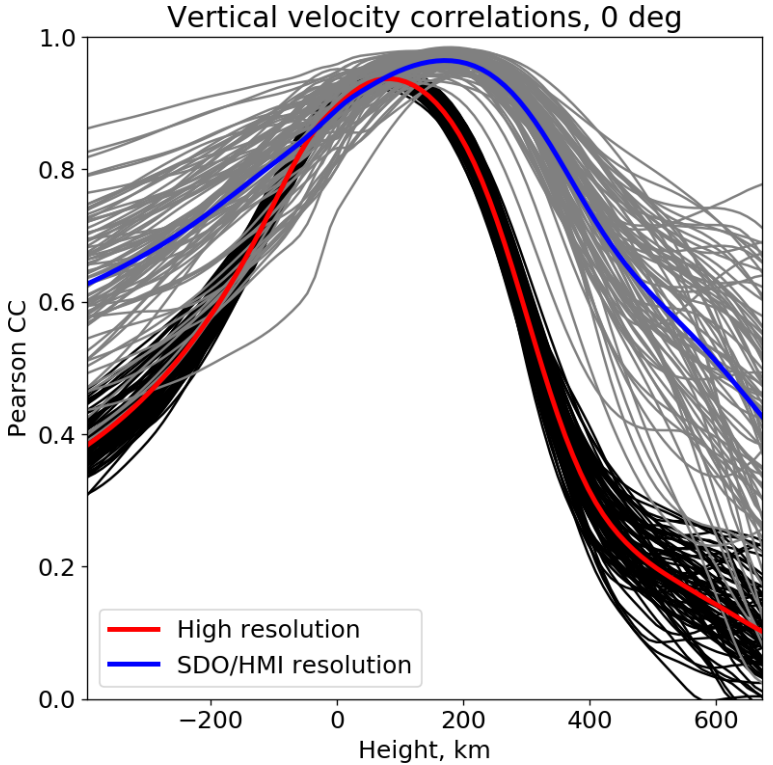

Pearson correlation coefficient between the line-of-sight velocity observable and corresponding physical properties of the atmosphere for the solar disk center case.

Observables and Atmospheric Properties

- To understand to which height of the atmosphere the observables are sensitive to, we calculate Pearson CC between the observables and the actual physical properties
- The line-of-sight velocity observables are unambiguously correlated with the physical quantities at certain heights for the disk center case (there is a sharp peak of the CC)
- The same is true for v_{LOS} for cases of other projection angles

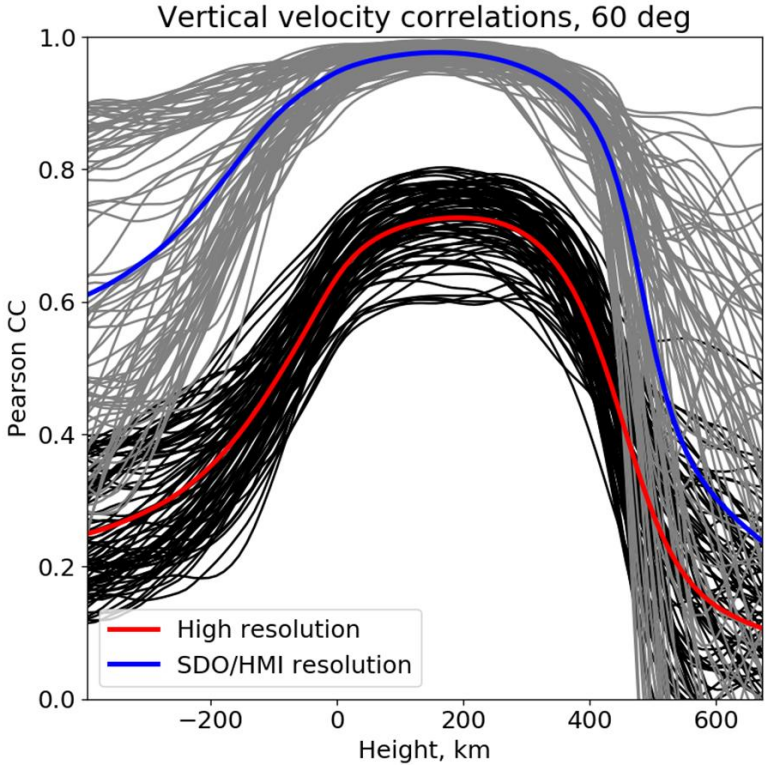

Pearson correlation coefficient between the line-of-sight velocity observable and corresponding physical properties of the atmosphere for 60 deg away from the solar disk center.

Observables and Atmospheric Properties

- To understand to which height of the atmosphere the observables are sensitive to, we calculate Pearson CC between the observables and the actual physical properties
- The line-of-sight velocity observables are unambiguously correlated with the physical quantities at certain heights for the disk center case (there is a sharp peak of the CC)
- The same is true for v_{LOS} for cases of other projection angles
- The situation is less evident for the B_{LOS} observable. The correlations are weaker and more ambiguous

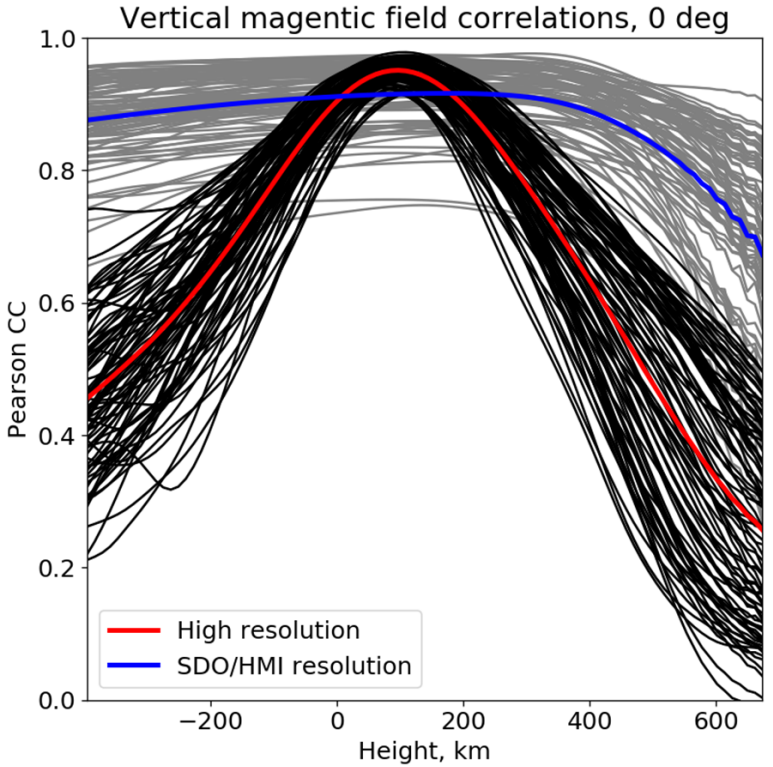

Pearson correlation coefficient between the line-of-sight magnetic field observable and corresponding physical properties of the atmosphere for the solar disk center case.

Observables and Atmospheric Properties

- To understand to which height of the atmosphere the observables are sensitive to, we calculate Pearson CC between the observables and the actual physical properties
- The line-of-sight velocity observables are unambiguously correlated with the physical quantities at certain heights for the disk center case (there is a sharp peak of the CC)
- The same is true for v_{LOS} for cases of other projection angles
- The situation is less evident for the B_{LOS} observable. The correlations are weaker and more ambiguous

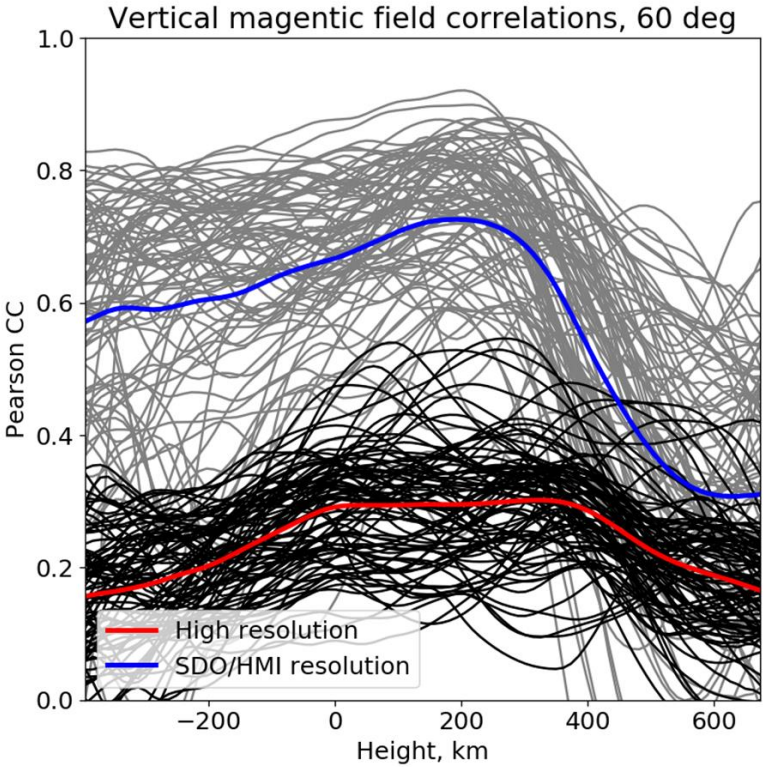

Pearson correlation coefficient between the line-of-sight magnetic field observable and corresponding physical properties of the atmosphere for 60 deg away from the solar disk center.

Angular Dependence

Summary of the correlation results:

- The height corresponding to the strongest correlations increases with the projection angle for the V_{LoS} and B_{LoS} computed with high (numerical) resolution
- The SDO/HMI resolution observables are sensitive to mostly the same heights up until the 60-degree projection angle.

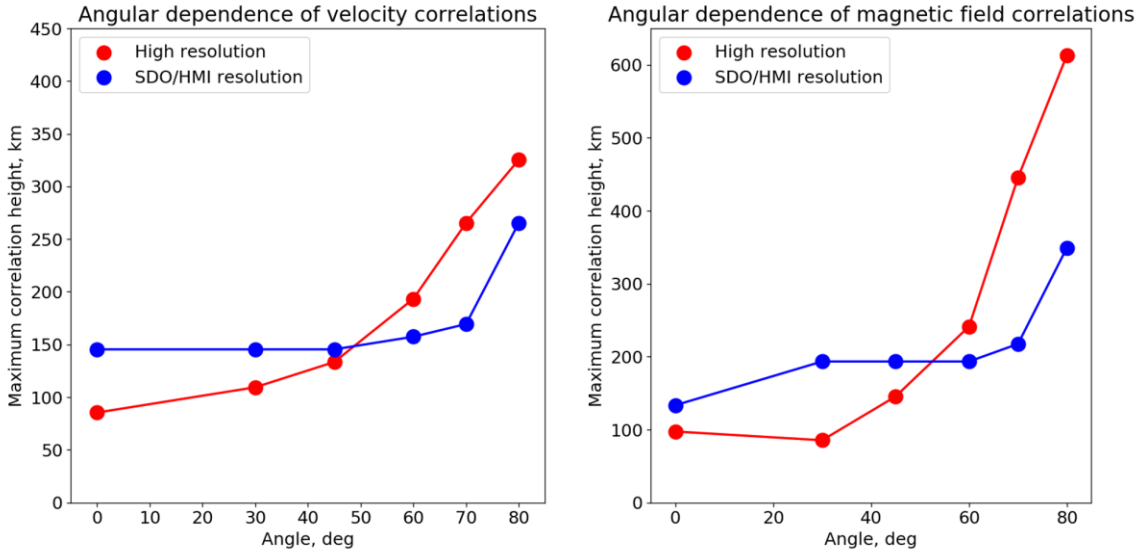

The heights of the strongest correlation between the V_{LoS} and V_{LoS} observable (left), and the B_{LoS} and B_{LoS} observable (right) as functions of the projection angle. The red curve corresponds to high-resolution observables, blue curves – to SDO/HMI resolution observables.

Integrated Magnetic Fluxes and Intensities

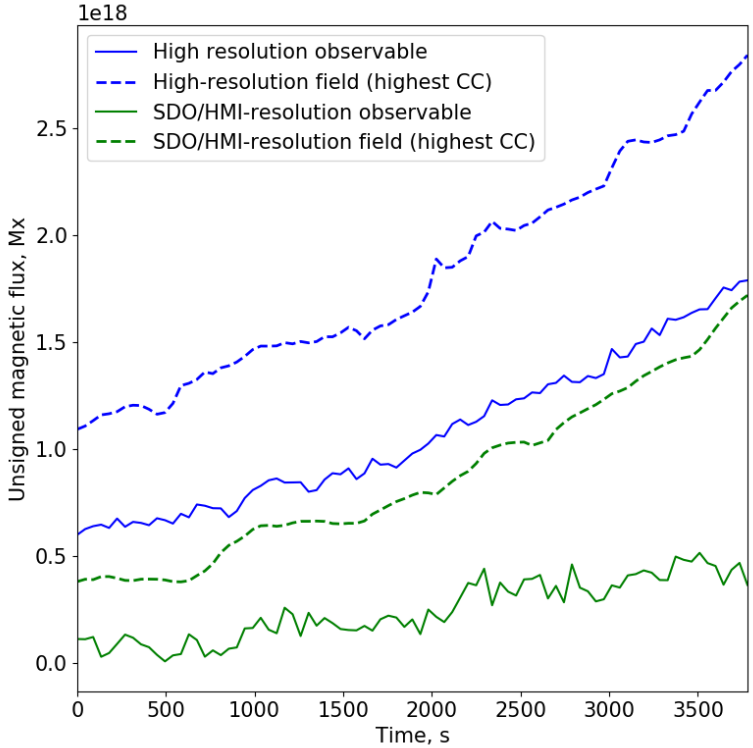

Integrated unsigned vertical magnetic flux computed from SDO/HMI observables (solid) and the magnetic field values at the strongest CC heights (dashed) for the disk center case

We also compare the integrated unsigned magnetic flux and the continuum intensity derived from observables with their actual values (the magnetic fields at the strongest correlation heights, and the continuum intensity computed from resolved line profiles)

- The integrated unsigned magnetic flux calculated from the observables underestimates the actual flux at the strongest correlation heights by about 40% on average.
- The integrated continuum intensity calculated from the observables is about 5-8% larger than its actual value (recovered from the resolved Stokes profiles)

Integrated Magnetic Fluxes and Intensities

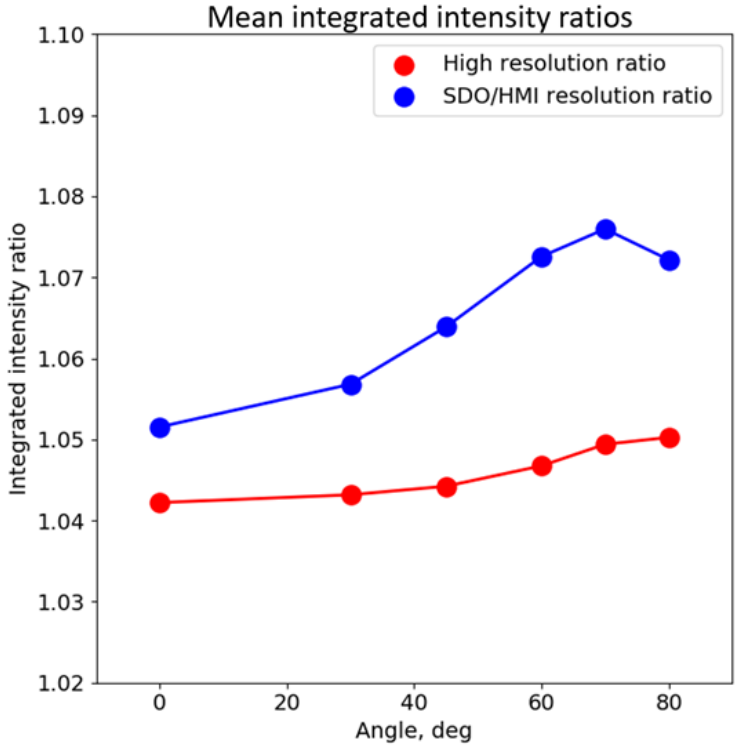

A comparison of the ratio of the integrated continuum intensity observable to the actual integrated continuum intensity as functions of the projection angle

We also compare the integrated unsigned magnetic flux and the continuum intensity derived from observables with their actual values (the magnetic fields at the strongest correlation heights, and the continuum intensity computed from resolved line profiles)

- The integrated unsigned magnetic flux calculated from the observables underestimates the actual flux at the strongest correlation heights by about 40% on average.
- The integrated continuum intensity calculated from the observables is about 5-8% larger than its actual value (recovered from the resolved Stokes profiles)

Radial Velocity Analysis

- Using the developed pipeline, we can also simulate the effect of the orbital radial velocities of the SDO spacecraft on the observables

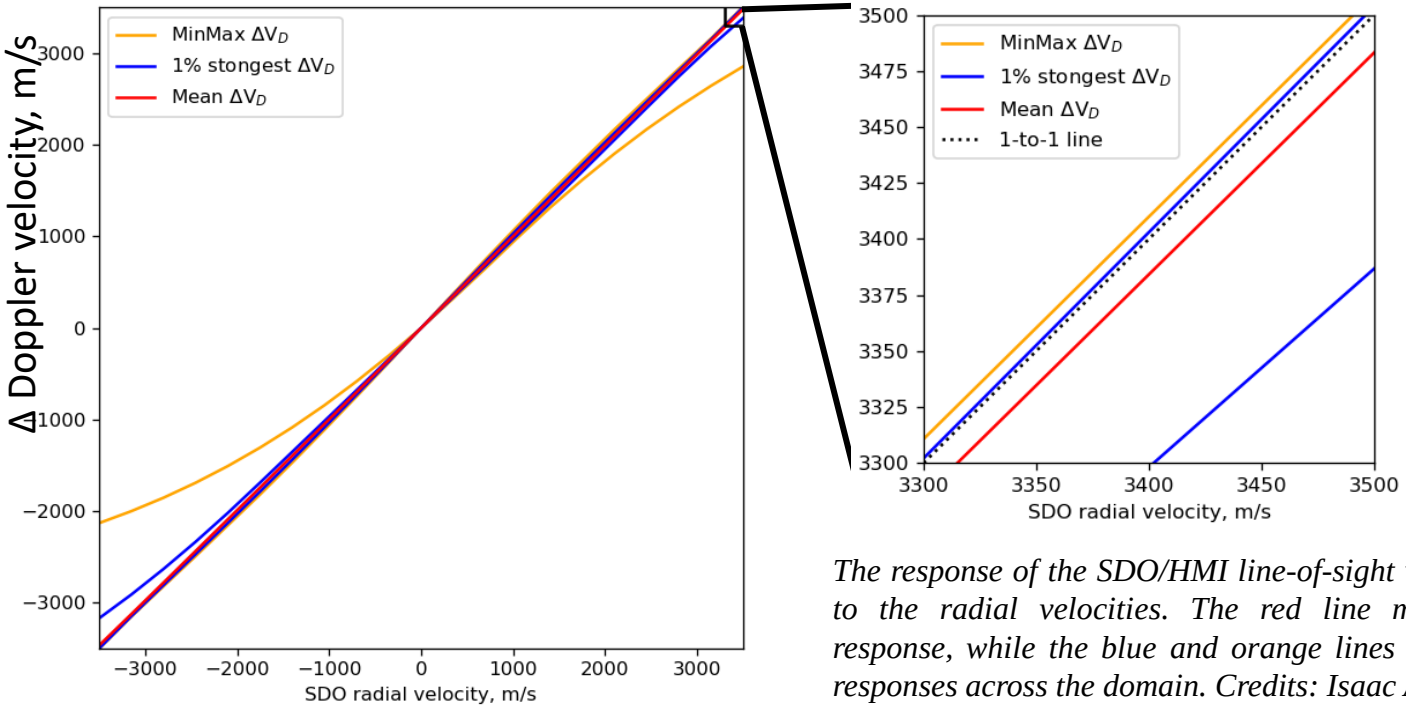

The response of the SDO/HMI line-of-sight velocity observable to the radial velocities. The red line marks the average response, while the blue and orange lines mark the strongest responses across the domain. Credits: Isaac Asante, GSU

Conclusions

- The combination of the realistic simulations and radiative transfer modeling is a powerful tool for providing interpretation of spectro-polarimetric observations of the solar atmosphere
- Modeling of the SDO/HMI velocity and magnetic field measurements of the quiet-Sun regions allowed us to accurately determine the effective heights of the observed properties for different distances from the disk center, investigate the center-to-limb variations and improve the calibration of these measurements.
- For high-resolution observations, the observing heights increase from about 100 km above the photosphere for observations at the disk center to 300-600 km at 80 degrees from the disc center.
- For the observations with the SDO/HMI resolution, the heights are relatively stable at ~150-200 km. The total unsigned magnetic flux in the HMI observations of quiet-Sun regions is underestimated by about 40%, while the continuum intensity is overestimated by about 5-8%

This work is supported by NSF grants 1835958 and 1936361, and NASA COFFIES DSC grant.